SCIENCE CHINA
Physics, Mechanics & Astronomy

• Research Paper •

July 2010 Vol. 53 No. 7: 1234–1238
doi: 10.1007/s11433-010-4014-1

Photonic Feshbach resonance†

XU DaZhi[1,2],LAN Hou[1], SHI Tao[1], DONG Hui[1*] & SUN ChangPu[1*]

[1]*Institute of Theoretical Physics, Chinese Academy of Sciences, Beijing 100190, China;*
[2]*Department of Modern Physics, University of Science and Technology of China, Hefei 230026, China*

Received March 24, 2010; accepted April 8, 2010; published online June 7, 2010

Feshbach resonance is a resonance for two-atom scattering with two or more channels, in which a bound state is achieved in one channel. We show that this resonance phenomenon not only exists during the collisions of massive particles, but also emerges during the coherent transport of massless particles, that is, photons confined in the coupled resonator arrays linked by a separated cavity or a tunable two level system (TLS). When the TLS is coupled to one array to form a bound state in this setup, the vanishing transmission appears to display the photonic Feshbach resonance. This process can be realized through various experimentally feasible solid state systems, such as the couple defected cavities in photonic crystals and the superconducting qubit coupled to the transmission line. The numerical simulation based on the finite-different time-domain (FDTD) method confirms our assumption about the physical implementation.

Feshbach resonance, bound state, single-photon transistor

PACS: 42.72.-g, 74.81.Fa, 73.43.Nq

1 Introduction

Feshbach predicted many years ago [1] that when two nuclei are scattered within an open entrance channel, they may enter the locally bounded state in the closed channel. If the relative kinetic energy of the input particle is fine-tuned to match the energy of the bound state, then the open channel and the closed channel resonate, so that the scattering length becomes divergent [2]. This resonance phenomenon is now called Feshbach resonance, which has been found in many physical systems over the years, such as the electron scattering of atoms [3], diatomic molecules [4] and ultra-cold atoms [5–7] and Bose-Einstein condensates (BEC) [2,8]. These experiments have helped to verify the simulation of various theoretical predictions in solid state systems [9], and in particular exemplifies the resonance phenomenon as a means for adjusting inter-atomic coupling in realizing various quantum phases ranging from BEC to BCS [10, 11].

On the other hand, the emergence of bound states appearing in a continuum [13] has been studied [14] for various models [15–17] as a long-standing fundamental problem in quantum mechanics. Quasi-bound states have been predicted in tight-binding fermionic quantum wires [18] for localized fermions and in the optical coupled resonator arrays [12, 19, 20] for confined photons.

Various applications have been found in quantum optical devices [21–23], including the conceptual design of the single-photon transistor [24]. In retrospect, we ask if it is possible to control the transmission exactly when the photons become bounded and unbounded through an external parameter *viz.*, to implement an photonic version of Feshbach resonance, or all-optical Feshbach resonance. The desired resonance between the bound and the unbound states can be found inside a pair of parallelly placed coupled resonator arrays [12].

2 Model setup and bound states

In our model, as shown in Figure 1(a), the two arrays of cavity are connected by a central cavity that acts as a quantum controller, forming an H-shape system. We designate the upper array as Array A with the Hamiltonian

*Corresponding author (email: dhui@itp.ac.cn, suncp@itp.ac.cn)

†Contributed by SUN ChangPu

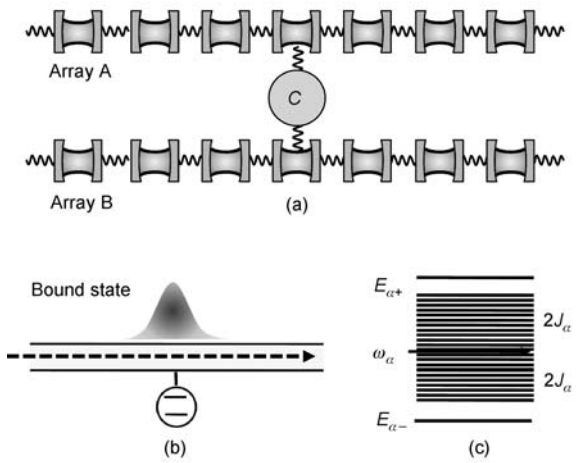

Figure 1 The all-optical Feshbach resonance in the coupled resonator system (a) with Array A and Array B, connected by a two level system or a central cavity. (b) A quasi-bound state of a single photon in an array. (c) The band structure of a spectrum for array α, $\alpha \in \{A, B\}$, with a discrete level above or below the energy band.

$$H_{\rm A} = \omega_{\rm A} \sum_j a_j^\dagger a_j + \left(J_{\rm A} \sum_j a_j^\dagger a_{j+1} + g_{\rm A} a_0 c^\dagger + {\rm h.c} \right), \quad (1)$$

where the second summation describes the tight-binding hopping of photons among cavities with the hopping coefficient $J_{\rm A}$. a_j denotes the annihilation operator of the bosonic mode for the j-th cavity field and we assume that the mode frequency $\omega_{\rm A}$ of each cavity field is identical. The last term is the interaction between the central cavity C with single mode frequency Ω and the zeroth resonator of Array A with coupling strength $g_{\rm A}$. $c^\dagger$ is the corresponding creation bosonic operator for the central cavity. The lower array is designated as Array B and as the Hamiltonian $H_{\rm B}$ which is not different from eq. (1) except the change of the bosonic mode operator to b_j, the hopping coefficient to $J_{\rm B}$, the mode frequency to $\omega_{\rm B}$ and the coupling strength to $g_{\rm B}$. Then, the total model Hamiltonian reads $H = H_{\rm A} + H_{\rm B} + \Omega c^\dagger c$. For single photon transfer, the central cavity takes the role as that of a two level system (TLS) with two levels $|e\rangle = |1\rangle$ and $|g\rangle = |0\rangle$. In this sense our construction can also be implemented through the circuit QED system [25] including two coupled superconducting transmission line cavity linked by charge or flux qubit.

For Array A, the eigenstate is assumed as $|\varphi_{\rm A}\rangle = \sum_j u_{{\rm A},g}(j) \left| g, 1_j, 0 \right\rangle + u_{{\rm A},e} |e, 0, 0\rangle$, where only the excited state of the central cavity and a single-photon excitation in one of the cavities are included. Corresponding to the probability amplitudes $u_{{\rm A},g}(j)$ and $u_{{\rm A},e}$ Array B takes similar states with coefficients $u_{{\rm B},g}(j)$ and $u_{{\rm B},e}$. To see whether there are bounded single-photon states within their individual coupled resonator array, we solve the discrete-coordinate scattering equation

$$[E - \omega_\alpha - V_\alpha(E)] u_{\alpha,g}(j) = -J_\alpha [u_{\alpha,g}(j+1) + u_{\alpha,g}(j-1)] \quad (2)$$

with eigenvalue E. Here the term

$$V_\alpha(E) = \frac{g_\alpha^2 \delta_{j0}}{E - \Omega} \quad (3)$$

on the left hand side is contributed by the interaction between the central cavity and the coupled resonator array. It appears that $V_\alpha(E)$ is a resonate potential dependent of the eigenenergy E. This δ-type potential forms a confining barrier to the transportation of single photon in the coupled resonator array and forms a bounded state of single photon, similar to those proposed in refs. [19,20]. It has a singularity at E being equal to the level spacing Ω, leading to a quasi-plane-wave type solution [12] to eq. (2), $u_{\alpha,g}(j) = C_\alpha \exp(-{\rm i}\kappa_\alpha |j|)$, where the wave number is complex, $\kappa_\alpha = \kappa_{\alpha,R} - {\rm i}\kappa_{\alpha,I}$. The imaginary part $\kappa_{\alpha,I}$ of the wave number admits a positive value and for the non-zero coupling g_α, results in a decay of the probability distribution of single-photon states over the discrete spatial coordinate j. The vanishing probability amplitude towards the ends of the arrays, i.e. along with $|j| \to \infty$, demonstrates the existence of a bound state of a single photon, as shown in Figure 1(b). In this system, the continuum band has a bandwidth $4J_\alpha$ and its paired discrete levels, denoted respectively by $E_{\alpha+}$ and $E_{\alpha-}$, are gapped from either below or above, as illustrated in Figure 1(c). In the conventional language of atomic scattering, the continua of eigenenergies can be considered as open channels of multiple admissible energy states in the continuous range $\omega_\alpha - 2J_\alpha < E < \omega_\alpha + 2J_\alpha$. Out of this range, the energy states can only admit two discrete levels that are associated with a non-real k_α, representing closed channels or bound states with energies

$$E_{\alpha\pm} = \Omega \pm \frac{g_\alpha^2}{\sqrt{(E_{\alpha\pm} - \omega_\alpha)^2 - 4J_\alpha^2}}. \quad (4)$$

The similar bound state equation can also be found in refs. [15–17].

3 Resonate scattering

The scattering state $|\varphi\rangle$ of the two-chain system for single-photon reads

$$|\varphi\rangle = \sum_j \left[u_{{\rm A},g}(j) \left| g, 1_j, 0 \right\rangle + u_{{\rm B},g}(j) \left| g, 0, 1_j \right\rangle \right] + u_e |e, 0, 0\rangle . \quad (5)$$

The amplitudes $u_{{\rm A},g}(j)$, $u_{{\rm B},g}(j)$and u_e can still be analyzed through the time-independent Schrödinger equations, leading to a pair of algebraic scattering equations similar to eq. (2). The distinction of the case here lies in adding

$$W_\alpha(E) = \frac{g_\alpha g_{\bar\alpha} u_{\bar\alpha,g}(0)}{E - \Omega} \quad (6)$$

on the right hand side with α= A or B. We have used $\bar\alpha$ to indicate the dual array relative to α.

We consider the particular cases that a single photon is inserted into Array A from the left. The state of this single

photon in the array is then described by a plane wave, $u_{\rm A}(j) = \exp({\rm i}kj) + R\exp(-{\rm i}kj)$ $(j < 0)$; $S\exp({\rm i}kj)$ $(j > 0)$. S and R denote, respectively, the transmission and the reflection coefficients of the optical plane wave, indicating the scattering of photon by the effective potential at the zeroth resonator in the one-dimensional coordinate space. Meanwhile, the distribution amplitude for the single photon in Array B can be quasi-plane-wave type, $u_{\rm B}(j) = C_{\rm B}\exp\{-{\rm i}\kappa|j|\}$, with a complex wave number κ, and indicates a closed channel, identical to that of the individually discussed case. The coupled scattering equations give rise to our main result

$$(1-S)\frac{\sin kJ_{\rm A}}{g_{\rm A}} = \frac{\sin\kappa C_{\rm B}J_{\rm B}}{g_{\rm B}} = \frac{g_{\rm A}S + g_{\rm B}C_{\rm B}}{2{\rm i}(\Omega - E)}. \tag{7}$$

Therefore, the optical dual-channel resonance occurs when there exists a solution of real k and complex κ to eq. (7) and the eigenenergy E of the photon in Array A matches either of the discrete energy levels $E_{\rm B\pm}$ of Array B. The process is illustrated in Figure 2 for two particular cases with E matching $E_{\rm B+}$ in Figure 2(a) or $E_{\rm B-}$ in Figure 2(b).

The criteria of the dual-channel resonance can be met if the transmission coefficient S in eq. (7) vanishes. This condition implies the circumstance where the incident photon in Array A is totally reflected or scattered by the potential barrier set up by the central cavity at position $j = 0$. It follows from

$$S = -\frac{C_{\rm B}}{g_{\rm A}g_{\rm B}}\left[2J_{\rm B}(E-\Omega)\sin\kappa - g_{\rm B}^2\right] \tag{8}$$

that the transmission coefficient vanishes when $E = \Omega - g_{\rm B}^2/(2{\rm i}J_{\rm B}\sin\kappa)$, leading to a complex wave number κ as expected. The complete reflection in the open channel can be understood as the divergence effect of s-wave scattering length for the usual atomic Feshbach resonances in three-dimensional space reduced to a version in one-dimensional space.

As a function of the incident energy E, the transmission coefficient

$$S = \begin{cases} \frac{F_{\rm A}(E)}{F_{\rm A}(E)-G_-(E)}, & E > \omega_{\rm B} + 2J_{\rm B}, \\ \frac{F_{\rm A}(E)}{F_{\rm A}(E)-G_+(E)}, & E < \omega_{\rm B} + 2J_{\rm B} \end{cases} \tag{9}$$

is re-written in terms of $F_\alpha(E) = \sqrt{(E-\omega_\alpha)^2 - 4J_\alpha^2}$ for $\alpha = {\rm A}, {\rm B}$ and

$$G_\pm(E) = \frac{g_{\rm A}^2 F_{\rm B}(E)}{(E-\Omega)F_{\rm B}(E) \pm g_{\rm B}^2}. \tag{10}$$

The norm-squared reflection coefficient $|R|^2 = |1-S|^2$ is plotted against the photon energy in families of varying level spacing Ω and coupling constant $g_{\rm A}$ of the TLS in Figure 3. The photon encounters two kinds of characteristic points while propagating through Array A. The first one is an indifferentiable turning point where $S = 1$ or $E = \omega_{\rm B} + 2J_{\rm B}$. The potential barrier becomes transparent and the photon is completely transmitted because of the matching coupling between the TLS controller and the dual Array B. The second one is the maximum point where the photon is fully reflected when the transmission coefficient is vanishing $S = 0$. We hence see the shifting of this peak while Ω is varied. The reliance on the coupling coefficient $g_{\rm A}$ determines the width of the peaking.

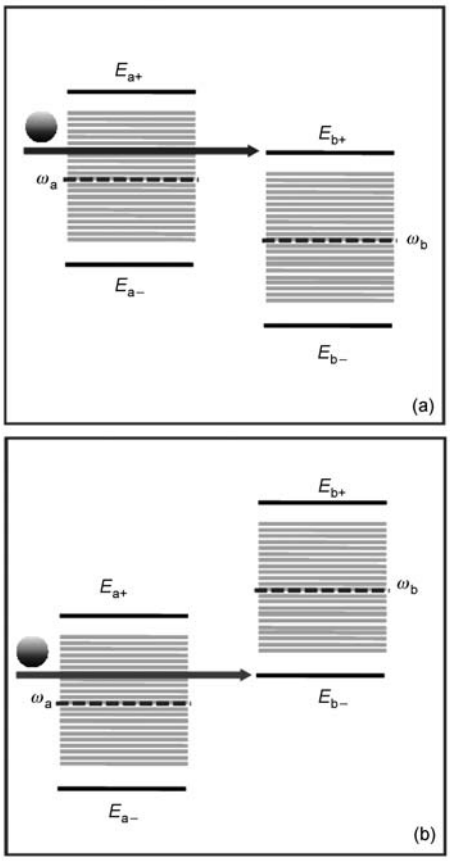

Figure 2 The diagrams of the energy spectra of the single photon in Array A and Array B. Two particular resonance cases exist for an incident photon inserted into Array A: (a) The photon energy level in the band in Array A is resonant with the upper discrete level in Array B; (b) the photon energy level in the band in Array A is resonant with the lower discrete level in Array B.

4 Numerical simulations based on finite-difference time-domain approach

Next we numerically examine the feasibility of our theoretical prediction of a two-dimensional photonic crystal [26,27]. This artificial crystal is made up of a square lattice of high-index dielectric rods of radii $0.2a$, $0.1a$ and $0.05a$, where a is the lattice spacing. The artificial design consists of two parallel waveguides of coupled defected cavity arrays linked through a central defected cavity on the two-dimensional photonic crystal, as illustrated in Figure 4(a). The two resonator arrays [28] are constructed with different frequencies, inter-resonator tunneling constants, and coupling strengths with the central cavity.

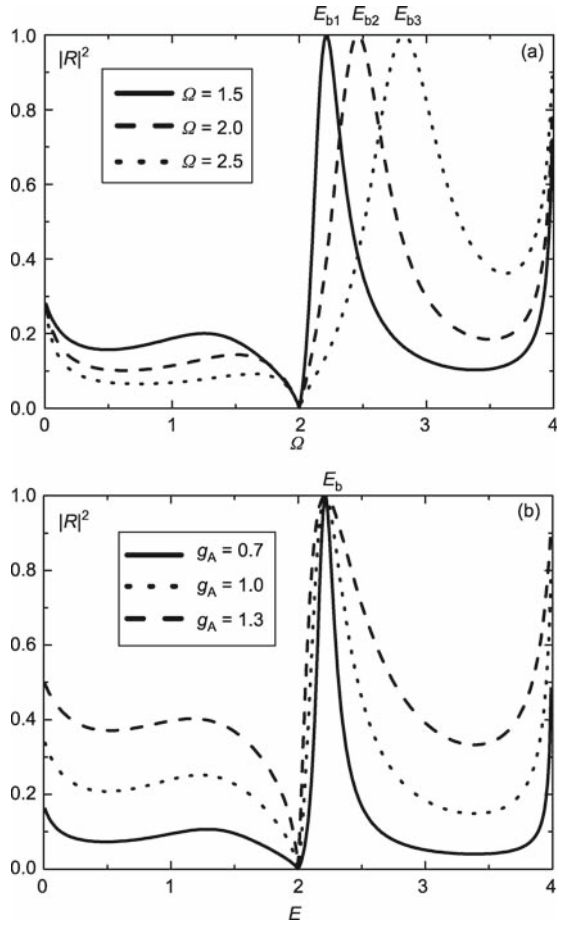

Figure 3 Plots of the norm-squared reflection coefficient $|R|^2$ against the eigenenergy E of a propagating photon. Two tuning parameters are varied: (a) the level spacing Ω of the TLS controller; and (b) the coupling coefficient g_A. Other parameters are $J_A = 1$, $J_B = 0.5$, $\omega_A = 2$, $\omega_B = 1$ and $g_B = 0.7$. The incident energy ranges from 0 to 4 and the continuum band for Array B is set $[0, 2]$. The corresponding bound state energies are marked as E_{b1}, E_{b2}, E_{b3} in (a) and E_b in (b).

For this photonic crystal, the materials of all the rods are assumed to be silicon, with a dielectric constant $\epsilon = 11.56$, and the background is filled by air. We make the simulation of the designed structure with the finite-difference time-domain (FDTD) method [29] in the freely available Meep code [30]. The steady distribution of Ez field for transverse magnetic (TM) wave at a frequency $\omega_0 = 0.3628 \times 2\pi c/a$ is plotted in Figure 4(b) which shows the magnitudes of the amplitudes.

The notice-worthy region is located at the center where the highly-saturated colors indicate a localized bounded photon from the lower waveguide. Moreover, the blank portion in the upper waveguide indicates a completely reflected wave. The numerical results show that the total reflection indicating Feshbach resonance, indeed occurs by accompanying the formation of bound states. We point out that, though the numerical simulation based on FDTD is classical essentially, the weak light calculation can also reflect the single photon nature with the intensity distribution illustrated in Figure 4(b), which is only relevant to the first order coherence function.

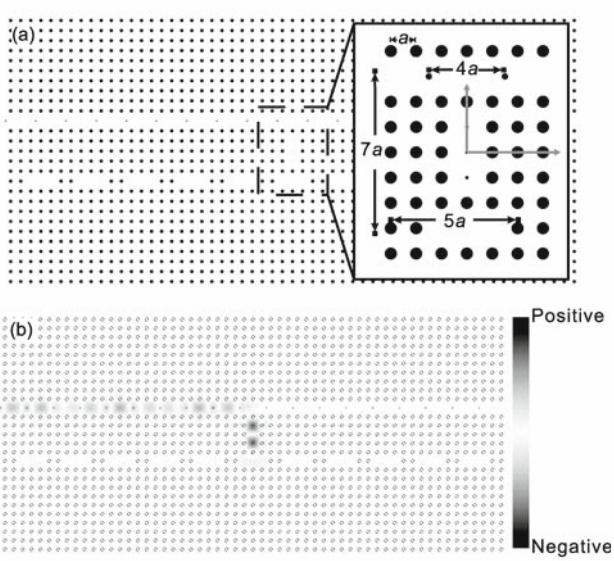

Figure 4 An experimental protocol based on a photonic crystal made up of silicon rods of radius $0.2a$. (a) The setup of practical design: the upper waveguide is implemented by removing a row of original rods and substituting them with a set of rods of radii $0.1a$ and spacing $d_{UP} = 4a$. The lower waveguide with $7a$ apart from the upper one is constructed by removing three rods out of every five rods with lattice spacing $d_{DOWN} = 5a$. The central cavity is created by reducing the radius of three vertically-placed rods between the two waveguides to $0.05a$. (b) Plotting the steady electric field vector for an incident wave of frequency $\omega_0 = 0.3628 \times 2\pi c/a$ with TM-polarization.

5 Conclusion

We have predicted an all-optical Feshbach resonance, which emerges from a pair of these coupled resonator arrays coupled in an H-shape fashion. It is shown that this resonance phenomenon is associated with the existence of photonic bound states in a TLS-controlled coupled resonator array. We have also carried out an FDTD simulation of the system to verify the validity of this prediction for the practical phonic crystal. Essentially, the resonance phenomenon arises from the dual-channel coupling between an unbound state in one array and a bound state in the other. Its moment of occurrence is indicated by a total reflection of an incident photon in the array. Our analysis of the resonant scattering process made for the single photon case, does not rely on the photonic statistics. The prediction here is, therefore, applicable to fermionic models, such as the electron transportation along an H-shape array of quantum dots. For the case of multiple photons transportation in the arrays, the Bethe-ansatz is needed for the analysis [31]. Most recently, an analytical approach based on the Lehmann-Symanzik-Zimmermann reduction [32] was demonstrated to be useful in studying the multi-photon effects (such as the bunching and anti-bunching phenomena) of scattering in the present setup.

SUN ChangPu acknowledges the helpful discussion with YANG Shuo, ZHANG Peng and WANG XueHua. This work was supported by the National Natural Science Foundation of China (Grant Nos.10474104, 60433050 and 10704023), and the National Basic Research Program of China (Grant Nos. 2006CB921205 and 2005CB724508).

1 Feshbach H. Unified theory of nuclear reactions. Ann Phys, 1958, 5: 357–390
2 Timmermans E, Tommasini P, Hussein M, et al. Feshbach resonances in atomic Bose C Einstein condensates. Phys Rep, 1999, 315: 199–230
3 Schulz G J. Resonances in electron impact on atoms. Rev Mod Phys, 1973, 45: 378–422
4 Schulz G J. Resonances in electron impact on diatomic molecules. Rev Mod Phys, 1973, 45: 423–486
5 Courteille P, Freeland R S, Heinzen D J, et al. Observation of a Feshbach resonance in cold atom scattering. Phys Rev Lett, 1998, 81: 69–72
6 Roberts J L, Claussen N R, Jr. Burke J P, et al. Resonant magnetic field control of elastic scattering in cold ^{85}Rb. Phys Rev Lett, 1998, 81: 5109–5112
7 Vuletic V, Kerman A J, Chin C, et al. Observation of low-field Feshbach resonances in collisions of Cesium atoms. Phys Rev Lett, 1999, 82: 1406–1409
8 Inouye S, Andrews M R, Stenger J, et al. Observation of Feshbach resonances in a Bose C Einstein condensate. Nature,1998, 392: 151–154
9 Jin D S, Regal C A. Proceedings of the International School of Physics Enrico Fermi, Course CLXIV. Amsterdam: IOS Press, 2008
10 Loftus T, Regal C S, Ticknor C, et al. Resonant control of elastic collisions in an optically trapped Fermi gas of atoms. Phys Rev Lett, 2002, 88: 173201
11 Zirbel J J, Ni K-K, Ospelkaus S, et al. Collisional stability of fermionic Feshbach molecules. Phys Rev Lett, 2008, 100: 143201
12 Zhou L, Gong Z R, Liu Y X, et al. Controllable scattering of a single photon inside a one-dimensional resonator waveguide. Phys Rev Lett, 2008, 101: 100501
13 von Neumann J, Wigner E. Uber merkwturdige diskrete Eigenwerte. Z Phys, 1929, 30: 465–467
14 Friedrich H, Wintgen D. Physical realization of bound states in the continuum. Phys Rev A, 1985, 31: 3964–3966
15 Lee T D. Some special examples in renormalizable field theory. Phys Rev, 1954, 95: 1329–1334
16 Fano U. Effects of configuration interaction on intensities and phase shifts. Phys Rev, 1961,124: 1866–1878
17 Anderson P W. Localized magnetic states in metals. Phys Rev, 1961, 124: 41–53
18 Nakamura H, Hatano N, Garmon S, et al. Quasibound states in the continuum in a two channel quantum wire with an adatom. Phys Rev Lett, 2007, 99: 210404
19 Gong Z R, Ian H, Zhou L, et al. Controlling quasibound states in a one-dimensional continuum through an electromagnetically-induced-transparency mechanism. Phys Rev A, 2008, 78: 053806
20 Dong H, Gong Z R, Ian H, et al. Intrinsic cavity QED and emergent quasinormal modes for a single photon. Phys Rev A, 2009, 79: 063847
21 Shen J T, Fan S. Coherent single photon transport in a one-dimensional waveguide coupled with superconducting quantum bits. Phys Rev Lett, 2005, 95: 213001
22 Shen J T, Fan S. Strongly correlated two-photon transport in a one-dimensional waveguide coupled to a two-level system. Phys Rev Lett, 2007, 98: 153003
23 Shen J T, Fan S. Coherent photon transport from spontaneous emission in one-dimensional waveguides. Opt Lett, 2005, 30: 2001–2003
24 Chang D E, Sørensen A S, Demler E A, et al. A single-photon transistor using nanoscale surface plasmons. Nat Phys, 2007, 3: 807–812
25 Wallraff A, Schuster D I, Blais A, et al. Strong coupling of a single photon to a superconducting qubit using circuit quantum electrodynamics. Nature, 2004, 431: 162–167
26 Fan S. Sharp asymmetric lineshapes in side-coupled waveguide-cavity systems. Appl Phys Lett, 2002, 80: 908–910
27 Joannopoulus J D, Johnson S G, Winn J N, et al. Photonic Crystal: Molding the flow of light. Princeton University: Princeton University Press, 2007
28 Yariv A, Xu Y, Lee R K, et al. Coupled-resonator optical waveguide: A proposal and analysis. Opt Lett, 1999, 24: 711–713
29 Taflove A, Hagness S C. Computational Electrodynamics: The Finite-Difference Time-Domain Method. Artech: Norwood, MA, 2000
30 Farjadpour A, Roundy D, Rodriguez A, et al. Improving accuracy by subpixel smoothing in the finite-difference time domain. Opt Lett, 2006, 31: 2972–2974, http://ab-initio.mit.edu/wiki/index.php/Meep
31 Shen J T, Fan S. Strongly correlated multiparticle transport in one dimension through a quantum impurity. Phys Rev A, 2005, 76: 062709
32 Shi T, Sun C P. Lehmann-Symanzik-Zimmermann reduction approach to multiphoton scattering in coupled-resonator arrays. Phys Rev B, 2009, 79: 205111